Structure of light exotic nuclei ^{6,8}He and ^{10,11}C from (p,p') reactions

V. Lapoux, N. Alamanos, F. Auger, A. Drouart, A. Gillibert, C. Jouanne, G. Lobo, L. Nalpas, A. Obertelli, E. Pollacco, et al.

Structure of light exotic nuclei ^{6,8}He and ^{10,11}C from (p,p') reactions.

V. Lapoux[a*], N. Alamanos[a], F. Auger[a], A. Drouart[a], A. Gillibert[a], C. Jouanne[a], G. Lobo[a], L. Nalpas[a], A. Obertelli[a], E. Pollacco[a], R. Raabe[a], F. Skaza[a], J-L. Sida[a], D. Beaumel[b], E. Becheva[b], Y. Blumenfeld[b], F. Delaunay[b], L. Giot[c], E. Khan[b], A. Lagoyannis[d], A. Musumarra[e], P. Navràtil[f], A. Pakou[d], P. Roussel-Chomaz[c], H. Savajols[c], J-A. Scarpaci[b], S. Stepantsov[g], R. Wolski[g] and T. Zerguerras[b].

[a]CEA-Saclay,DSM/DAPNIA/SPhN F-91191, Gif-sur-Yvette, France

[b]IPN-Orsay, IN2P3-CNRS, 91406 Orsay Cedex, France

[c]GANIL, Bld Henri Becquerel, BP 5027, F-14021, Caen, France

[d]Dpt of Physics, Univ. of Ioannina, 45110 Ioannina, Greece

[e]INFN-Laboratori Nazionali del Sud, Via S. Sofia 44, 95123 Catania Italy

[f]LLNL, L-414, P.O.Box 808, Livermore, California 94551

[g]JINR, FLNR Dubna 141980 Dubna, Moscow region, Russia.

The structure of the light unstable nuclei ^{10,11}C and ^{6,8}He is investigated by means of (p,p') reactions. The experiments were performed at GANIL using the MUST detector, an array of Si and SiLi telescopes. The (p,p') are analyzed within the framework of the microscopic JLM potential, allowing to test the densities predicted by structure models. Preliminary data from the ^{8}He(p,p') reaction performed at the SPIRAL facility at 15.6 MeV/nucleon are discussed.

1. STRUCTURE OF UNSTABLE LIGHT NUCLEI

The main feature encountered by overviewing the nuclear chart in the light-mass region is the competition between mean field and correlations producing new "exotic" structures like neutron haloes found in ^{6}He, ^{11}Li [1,2] or alpha-clustering shapes [3]. For instance, the proton distribution of all the carbon isotopes are calculated to be oblate deformed in the Antisymmetrized Molecular Dynamics (AMD) framework [4], and the neutron deficient isotopes ^{9}C and ^{10}C are found with a well deformed prolate shape while triaxiality is predicted for the following odd isotope ^{11}C. In the light-mass region the stability is related to a complex interplay between mean field and correlation effects. A typical example is given by the He isotopes : ^{6,8}He are slightly bound, ^{5,7}He being unbound. Calculating their binding energy *ab initio* is a difficult task. Recent attempts were done with improved 3-body forces leading to a significant improvement over earlier descriptions [5]. No core

*E-mail: vlapoux@cea.fr

shell model calculations were also developed in the last few years and applied to light p-shell nuclei. They give relatively good results for the spectroscopy of the neutron-rich nuclei [6]. In particular, ^{8}He offers the possibility to study the effective Nucleon-Nucleon interaction in a portion of very-neutron rich and low-density nuclear matter (N/Z=3) ; the four-neutron separation energy is of 3.1 MeV only, and the ^{8}He nucleus, although having more neutrons than ^{6}He, has almost the same size, with a matter root mean square (rms) of 2.5 $\pm$ 0.1 fm, as deduced from the few-body analysis of the elastic scattering [7] or reaction cross sections [8]. We are dealing with a weakly bound nucleus with no bound excited states and low-lying resonances [9]. Within the five-body COSMA model [10], ^{8}He is described as an inert alpha core with four valence neutrons occupying a full $0p_{3/2}$ subshell and constituting a neutron skin.
In order to investigate the structure of ^{10,11}C and ^{6,8}He we have measured (p,p') scattering. Our aim is to obtain information on the spatial repartition of the nucleons of exotic nuclei, namely the densities, ground state and transition densities to excited states. We use the densities predicted by the microscopic models (either cluster or mean field models) to calculate the (p,p') angular cross sections and compare them to the experimental data. The analysis of the reaction will provide constraints on the models predicting cluster structures. The analysis of the ^{10,11}C(p,p') results can be found in Ref. [11].

1.1. (p,p') probe

The nucleon-nucleus potential used in this study is the microscopic, complex and parameter-free JLM potential [12], parameterized for incident energies up to 160 MeV. It depends only on the incident energy E and on the neutron and proton densities of the nucleus. In general, it is written using λ_V and λ_W the normalization factors for the real and imaginary parts. For A $\geq$ 20, λ_V and λ_W can be slightly modified (less than 10%) to fit the nucleus-nucleon data, but they are close to 1 for all A $\geq$ 20 stable nuclei. It was shown that usually in the case of light nuclei (A $\leq$ 20) $\lambda_W = 0.8$ [13]. We adopt it as the standard normalization of JLM for light nuclei. This potential allows a good reproduction of large sets of nucleon-nucleus data [13–15]. The inelastic (p,p') angular cross sections are obtained through Distorted Wave Born approximation (DWBA) calculations including the JLM potential. The entrance, transition and exit channel potentials are defined with the ground state and transition density. The normalization of the real and imaginary parts is fixed with the values obtained in the analysis of the elastic scattering. The calculated inelastic (p,p') cross sections are sensitive to the M_n and M_p factors, which are the radial moments of the transition densities : $M_{p,n} = \int drr^{l+2}\rho^{tr}_{p,n}$ with l the multipolarity of the transition. The M_p factor for a J_i to J_f transition is directly related to the corresponding B(El) transition strengh value obtained by Coulomb excitation experiments. We adopt here the following convention for the relationship between $|M_p|$ and B(E2) : $B(E2) = \frac{e^2}{(2J_i+1)}|M_p|^2$. The models of elastic and inelastic scattering on proton including the potential JLM were proven to be reliable to extract the fundamental quantities such as M_n/M_p without ambiguity for the stable nuclei [14] as well as for the exotic nuclei [15,16]. A careful analysis of the elastic scattering is required in the case of weakly-bound nuclei in order to have a correct treatment of the coupling effects, as will be explained in the following section.

1.2. Coupling effects

We have shown [17] that the angular distributions of ^{6}He on proton are better reproduced with a reduction of the real part of the JLM optical potential. The origin of this effect was discussed in Ref. [18] : in general, to calculate the interaction potential for elastic scattering, one should include all possible virtual couplings between the ground state and higher excited states. These processes remove flux from the elastic channel. This effect is negligible for stable nuclei, but becomes significant for weakly-bound nuclei. In particular for exotic isotopes with lower particle thresholds the coupling between the ground state and the continuum are expected to increase. The interaction term arising from couplings to inelastic channels is called the dynamical polarization potential (DPP). It is complex, non-local and energy-dependent. Its exact calculation requires the precise knowledge of the spectroscopy of the nucleus and of the transition strenghs to bound and continuum excited states. It is then difficult to evaluate and is not taken into account in the usual optical model approaches. It was explained in Ref. [19] that a complex surface potential, with a repulsive real part, is expected to simulate the surface effects generated by the DPP and this corresponds to the reduction of the real part. This effect is observed in the analysis with the JLM potential [17] of the ^{6}He + p scattering measured at 71 [20], 38.3 [17] and 25 [21,22] MeV/nucleon. By reducing the real part of the JLM potential we have reproduced successfully the whole set of data.

2. EXPERIMENTAL SET-UP

We measured elastic and inelastic scattering of ^{6,8}He isotopes on a proton target.

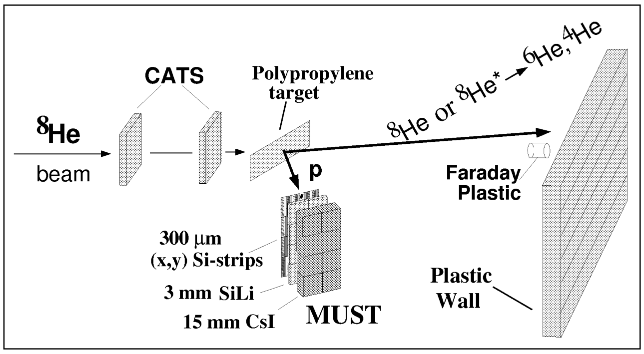

Figure 1. *Experimental set-up in the reaction chamber.*

For (p,p') reactions, the experimental apparatus MUST [23], an array of eight three-stage telescopes (a set of Si-strips, SiLi and CsI telescopes) specifically designed to detect recoiling light charged particles, is used to measure angular distributions for elastic and inelastic scattering of radioactive beams on proton target. We have measured recently at Ganil elastic and inelastic scattering of ^{8}He(p,p') using an ^{8}He beam produced by the SPIRAL facility at 15.6 MeV/nucleon with an intensity of 13000 part/s. The experimental set-up is described in Fig.1 in the case of the ^{8}He(p,p') reaction. The profile of the incident beam was given by two beam tracking detectors, the multi-wire chambers CATS [24]. Energy, time of flight (between MUST and CATS) and position of the light charged particle are measured in the MUST detector, allowing for an identification of the light particles and for a full reconstruction of the (p,p') kinematics. In coincidence with the ^{8}He heavy ejectile, it gives the elastic scattering, or with ^{6}He or ^{4}He coming from the 2^{+} unbound state of ^{8}He, it provides the determination of the inelastic scattering.

3. INELASTIC SCATTERING ^{6,8}He(p,p')

3.1. Investigation of the ^{6}He structure

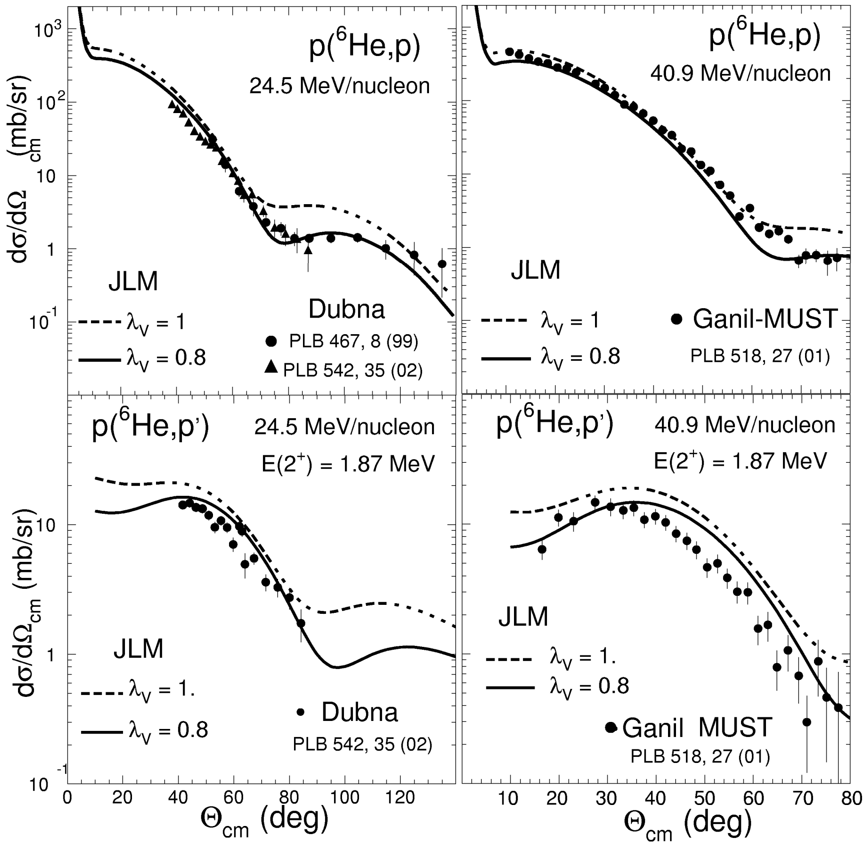

Figure 2. *Experimental and calculated cross sections for ^{6}He(p,p') at 24.5 and 40.9 MeV/nucleon. See details in the text.*

Using MUST, (p,p') scattering data to the first excited state of ^{6}He at 1.8 MeV were measured with a 40.9 MeV/nucleon ^{6}He beam produced by fragmentation of a primary ^{12}C projectile at 75 MeV/nucleon on the target of the SISSI device at Ganil [25]. The experimental results obtained at 40.9 [25] and 24 MeV/nucleon [22] can be compared with the calculated cross sections obtained using the JLM potential. Here we test the ground state (gs) and transition densities predicted in the 10 $\hbar w$ no-core shell model [6,26]. The gs density has a large matter rms radius of 2.5 fm, corresponding to the halo picture of this nucleus. The interaction potential tested on the elastic scattering is used in the calculation of the (p,p') scattering. The transition densities correspond to a B(E2) value of 1.06 e$^{2}.fm^{4}$, and to the ratio $|M_n|/|M_p| = 7.53$. In Fig. 2, the dashed and solid curves are calculations using the standard JLM and JLM with the reduced real part ($\lambda_V = 0.8$), according to our prescription (see 1.2), respectively.

3.2. Preliminary data for ^{8}He

The preliminary spectra obtained for the reaction of ^{8}He on the 44 mg/cm^2 thick polypropylene target are presented in Fig. 3. The figure on the left gives the reconstructed kinematics for the light protons and deutons and the figure on the right is the corresponding excitation spectrum for the (p,p') reaction. The energy of the proton or deuton detected in the MUST array is plotted as a function of the angle in the lab. frame. With the MUST wall located at 50° from the beam axis, the reactions are measured from 30° to 70° lab. The solid lines seen on the left plot are the calculated kinematical lines for ^{8}He(p,d)^{7}He and ^{8}He(p,p')(2$^+$, 3.6 MeV). The spectrum results from the data collected in all the MUST detectors.

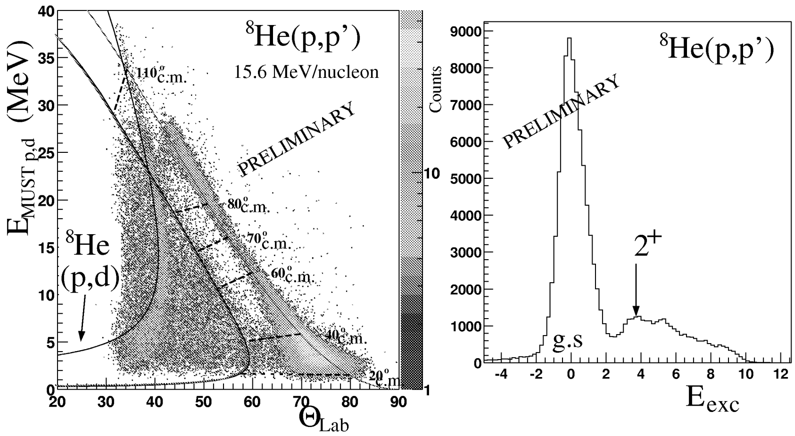

Figure 3. *Reconstructed kinematics for the inelastic scattering of ^{8}He on protons and (p,p') excitation spectrum. See details in the text.*

For the moment we have only preliminary data with the excitation spectrum showing the 2$^+$ excited state at 3.6 MeV and few bumps. Analysis is still in progress. The observed relative yields in the kinematical spectrum, for the elastic and the inelastic scattering to the 2$^+$, and for the (p,d) reaction are consistent with the observed magnitudes for the (p,p') and (p,d) cross sections measured previously at Riken, at 72 [9] and 35 [27] MeV/nucleon, respectively. The (p,d) reaction is enhanced in comparison with the (p,p') to the 2$^+$ state, which appears to be very weakly excited.

We will extract the experimental cross sections for (p,p') and (p,d) reactions and compare them to the theoretical distributions including densities for ^{8}He predicted either by few-body calculations, or calculated with no-core shell model, or with models based on realistic nucleon-nucleon interactions. This comparison will allow to validate or not the correlations between valence neutrons and alpha-core proposed by these models.

4. CONCLUSIONS

^{6,8}He(p,p') scattering data were measured using the MUST detectors. The aim of these experiments is to obtain structure information for these radioactive nuclei and to compare data to calculations performed with shell and few-body models predicting the ground state and transition densities. The ^{6}He(p,p') analysis was performed with the JLM potential. The potential in the entrance channel of this reaction was tuned on the elastic scattering. The coupling effects induced by the weak binding of the unstable nucleus ^{6}He on the interaction potential were taken into account by reducing the real part of the potential. The ^{6}He(p,p') results obtained at 40.9 MeV/nucleon, together with the 25 MeV/nucleon data have allowed to test and validate the transition densities predicted by the $10\hbar w$ shell model calculations. Ab initio no core shell model calculations have been performed recently [28] ; their predicted densities for ^{6,8}He will be tested by calculating the (p,p') scattering in the JLM approach and comparing them to the data. The aim is to explain the structure and the excitations of the Helium isotopes in order to better understand the correlations between core and neutrons.

REFERENCES

1. P. G. Hansen and B. Jonson, Europhys. Lett **4**, 409 (1987).
2. I. Tanihata, Nucl. Phys **A685** 80c (2001).
3. W. von Oertzen, Z. Phys. **A357**, 355 (1997).
4. Y. Kanada-En'yo and H. Horiuchi, Phys. Rev. C **55**, 2860 (1997).
5. R. B. Wiringa and S. C. Pieper, Phys. Rev. Lett **89**, 182501 (2002).
6. P. Navràtil and W. E. Ormand, Phys. Rev. C **57**, 3119 (1998).
7. J. S. Al-Khalili, J. A. Tostevin, Phys. Rev. C **57**, 1846 (1998).
8. J. A. Tostevin and J. S. Al-Khalili, Nucl. Phys **A616**, 418c (1997).
9. A.A. Korsheninnikov *et al.*, Phys. Lett. B **316**, 38 (1993).
10. M.V. Zhukov, A.A. Korsheninnikov and M.H. Smelberg, Phys. Rev. C **50** (1994) R1.
11. C. Jouanne, Paris VI University, PhD Thesis 2001, Internal Report CEA-Saclay, SphN-01-01T ; see C. Jouanne *et al.*, *VII International School-seminar on Heavy Ion Physics, Dubna (Russia), to be published in Yad. Fizika (Physics of Atomic Nuclei)* ; and to be submitted in Phys. Rev. C.
12. J. P. Jeukenne, A. Lejeune and C. Mahaux, Phys. Rev. C **16**, 80 (1977).
13. J. S. Petler *et al.*, Phys. Rev. C **32**, 673 (1985).
14. S. Mellema, R. Finlay, F. Dietrich and F. Petrovich, Phys. Rev. C **28**, 2267 (1983).
15. N. Alamanos, F. Auger, B. A. Brown and A. Pakou, J. Phys. G 24 (1998) 1541.
16. E. Khan *et al.*, Phys. Lett. B. **490** (2000) 45.
17. V. Lapoux *et al.*, Phys. Lett. B **517**, 18 (2001).
18. M.E. Brandan and G. R. Satchler, Phys. Rep. **285**, 143 (1997).
19. Y. Sakuragi, Phys. Rev C **35**, 2161 (1987).
20. A.A. Korsheninnikov *et al.*, Nucl. Phys. **A617**, 45 (1997).
21. R. Wolski *et al.*, Phys. Lett. B **467**, 8 (1999).
22. S. V. Stepantsov *et al.*, Phys. Lett. B **542**, 35 (2002).
23. The MUST collaboration, NIM A **421** (1999) 471-491.
24. S. Ottini *et al.*, NIM A **431**, 476 (1999).
25. A. Lagoyannis *et al.*, Phys. Lett. B **518**, 27 (2001).
26. E. Caurier, P. Navràtil, W.E. Ormand, J.P. Vary, Phys. Rev. C **64**, 051301 (2001).
27. A.A. Korsheninnikov *et al.*, Phys. Rev. Lett. **82**, 3581 (1999).
28. P. Nàvratil and W. E. Ormand, Phys. Rev. Lett. **88**, 152502 (2002).